Dalton Transactions

ROYAL SOCIETY OF CHEMISTRY

FRONTIER

View Article Online
View Journal | View Issue

Published on 01 April 2024. Downloaded by University of California - Davis on 1/16/2025 7:42:10 PM.

Check for updates

Cite this: *Dalton Trans.*, 2024, **53**, 6855

From Ln_2O_2S to $Ln_{10}OS_{14}$: exploring the sulphur spectrum of trivalent lanthanoid oxysulphides

Brian A. Wuille Bille† and Jesús M. Velázquez *

Received 31st January 2024,
Accepted 28th March 2024

DOI: 10.1039/d4dt00294f

rsc.li/dalton

While Ln_2O_2S oxysulphides have increasingly gained attention due to their structural and optoelectronic properties, an expansive compositional space lies beyond as the sulphur-to-oxygen ratio increases. In these oxysulphides, the compounded effect of the 4f states is manifold in the lanthanoid ions and the changing bonding and environment symmetry enables the tuning of their electronic structure and photophysical properties. Their challenging syntheses have made these materials largely unexplored, but recent efforts have been made to bridge the knowledge gap. In this article we present some of the structural characteristics and photophysical properties of the lanthanoid oxysulphide spectrum $Ln_xO_yS_z$.

Introduction

Lanthanoid oxysulphides, of general formula $Ln_xO_yS_z$, are a large class of materials with differing sulphur-to-oxygen ratios. Since the first elucidation of the structure of an oxysulphide in 1947,[1] these materials have been extensively studied due to their multitude of technological applications as colour-tunable phosphors,[2] sulphur-tolerant[3] catalyst supports for the water gas shift reaction,[4] and in magnetism[5] and luminescence thermal sensing.[6–9] While the compositional space is large, Ln_2O_2S has been the most widely explored stoichiometry,[10–12] and considerably less information is available on its remaining congeners.[13,14] The $Ln_2O_2S_2$ crystal structure was only recently understood owing to the disorder present in the disulphide layer.[15] Similarly, little is known about the mixed lanthanoid and solid solution ranges in the $Ln_{10}S_{15-x}O_x$ system and the impact the substitution of oxygen has on its crystal and electronic structures. Furthermore, for all compositions besides Ln_2O_2S, their photophysics are largely unknown.

In this article, we introduce the compositional spectrum of lanthanoid oxysulphides, summarize some of their salient properties and indicate where knowledge gaps reside. We emphasize the large opportunity for contributions to expand our limited knowledge of this exciting class of lanthanoid mixed anion materials.

Department of Chemistry, University of California, Davis, 95616, USA.
E-mail: jevelazquez@ucdavis.edu
† Present address: Department of Inorganic Spectroscopy, Max Planck Institute for Chemical Energy Conversion, Mülheim an der Ruhr, 45470, Germany.

Structural versatility

From Ln_2O_2S to $Ln_{10}OS_{14}$

In the large majority of lanthanoid oxysulphides, the cations adopt their most common +3 oxidation state, while the anions attain their −2 oxidation state, with the exception of $Ln_2O_2S_2$. Furthermore, due to their large ionic radius, the lanthanoid ions have high coordination numbers, typically between 7 and 8. In Ln_2O_2S, which crystallizes in the $P\bar{3}m1$ space group, the Ln^{3+} ions are coordinated by three S^{2-} and four O^{2-} in a capped trigonal antiprism along the *c*-axis, which results in a local C_{3v} symmetry (Fig. 1a). The oxydisulphides, Ln_2OS_2, of space group $P21/c$ demonstrate more asymmetric 7-fold coordination environments in their two distinct crystallographic sites (Fig. 1c). At the end of the spectrum, the highest sulphur content oxysulphide $Ln_{10}OS_{14}$ exhibits a tetragonal unit cell and a multitude of 8-fold coordinated crystallographic sites. Its atomic structure can be described as O-centred tetrahedra $[OLn_4]^{10+}$ surrounded by a "sea" of lanthanoid sulphide (Fig. 1d).[16] Different from the rest of the members, $Ln_2O_2S_2$ possesses a layered structured, in which fluorite-type $[Ln_2O_2]^{2+}$ units are separated by $(S_2)^{2-}$ dimers (Fig. 1b). Interestingly, the degree of disorder in the disulphide layer determines the specific crystal group (*Cmnce* or *I*4/*mmm*) as well as its topochemical reactivity.[15]

Cation substitution

Owing to the similarities in the lanthanoids' ionic radii, each oxysulphide crystal structure affords a large compositional space. Through the combination of different lanthanoid ions, a great variety of properties can be tailored. One such strategy involves doping, or the incorporation of small quantities, into the lattice of the host material. Well beyond the oxysulphides,

Published on 01 April 2024. Downloaded by University of California - Davis on 1/16/2025 7:42:10 PM.

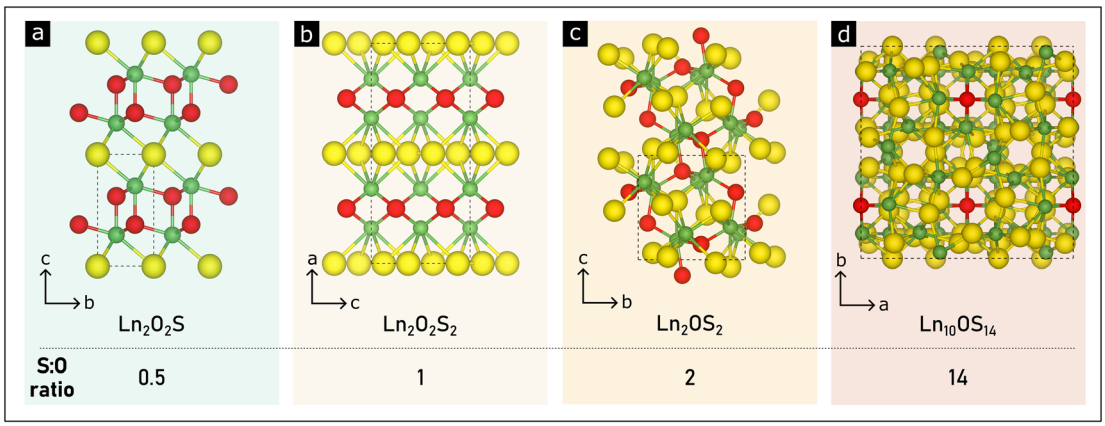

Fig. 1 Crystal structures of the lanthanoid oxysulphides and their S : O ratios. Unit cells are denoted with dashed lines. The green, red, and yellow circles represent Ln^{3+}, O^{2-}, and S^{2-}, respectively, represented with their atomic radii. Created with VESTA.[45]

doping with rare earth ions, most commonly the highly luminescent Eu, Er, Tb, and Yb, has been extensively used for the synthesis of enhanced luminescent semiconductors and nanoscintillators,[17] and in upconverted emission.[7,18] Oxysulphides can similarly act as hosts, with the benefits of high chemical stability, general low toxicity and high thermal sensitivity, characteristics that are especially important for their application in biological media and thermometry. Alternatively, binary, ternary and multinary lanthanoid oxysulphides can be synthesized. If the ionic radius tolerance is satisfied for the specific crystal structure, then more dramatic effects on its properties can be elicited by the combination of rare earth ions, like those observed in the band gap energies in a series of bimetallic $(Ce,Gd)_2O_2S$.[12] Therein, the band gap decreased progressively with Ce content, and so did its magnetic moment given the decrease in the number of 4f electrons of the lanthanoid ion (from $4f^7$ in Gd^{3+} to $4f^1$ in Ce^{3+}).[5] In addition, if these bimetallic oxysulphides are doped with a tertiary lanthanoid, even a finer modulation of the material properties can be achieved. Such is the example of $(Lu,Gd)_2O_2S:Tb^{3+}$ and $(Y,Gd)_2O_2S:Tb^{3+}$ systems, in which Lu and Y influence the energy transfer to the dopant ions, resulting in a greater colour change as a function of solid solution composition in the latter.[19] These strategies have paved the way for the exciting recent investigations into high-entropy oxysulphides that may unlock new reactivity and optoelectronics in this family of materials.[20,21]

Photophysics

Much like in oxynitrides and oxyhalides, the presence of mixed anions in oxysulphides enables the expression/enhancement of properties absent in their mono-anionic counterparts.[22,23] In particular, in terms of their photophysical properties, oxysulphides generally exhibit narrower bandgaps than their corresponding oxides. While structural differences certainly play a role in their band structures, in lanthanoid oxysulphides, valence band maxima are mostly of anion character, whereas the conduction band minima are dominated by lanthanoid 5d states (or transition metal d-states in multinary oxysulphides). Thus, the higher energy of the frontier sulphur orbitals leads to a rise in the valence band maximum, resulting in a decrease in the band gap energy. As a consequence, most lanthanoid oxysulphides are semiconductors with colours in the visible range of the electromagnetic spectrum (Fig. 2).

At first glance, both in Ln_2O_2S and $Ln_{10}OS_{14}$, there seems to be no clear trend in the measured optical band gap energies as a function of lanthanoid identity (Fig. 2b and c). Although the 4f orbitals tend to be unaffected by their chemical environ-

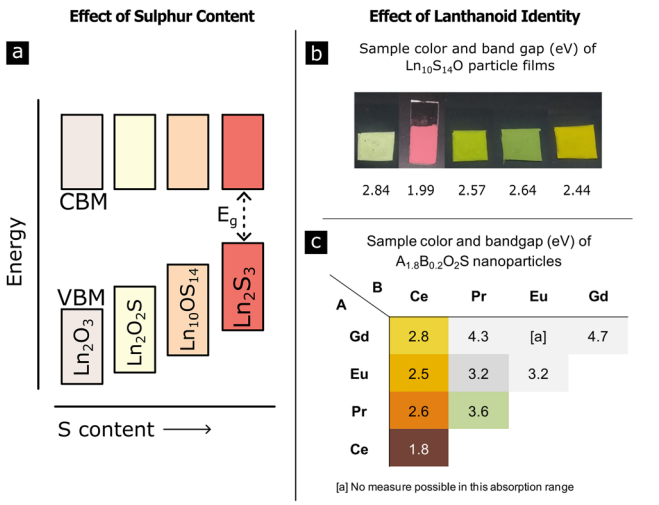

Fig. 2 Photophysical properties of lanthanoid oxysulphides: (a) qualitative block diagram of the progressive valence band edge maximum (VBM) rise as a function of sulphur content; (b) sample colour and band gap energy of $Ln_{10}S_{14}O$. Adapted with permission from ref. 14. Copyright 2022 by the American Chemical Society; (c) sample colour and band gap energy of Ln_2O_2S. Adapted with permission from ref. 12. Copyright 2019 by the American Chemical Society.

This journal is © The Royal Society of Chemistry 2024

Published on 01 April 2024. Downloaded by University of California - Davis on 1/16/2025 7:42:10 PM.

ment, their electrons interact with electromagnetic radiation, and they do so in rather complex manners.[24] In fact, the degree of covalency between the Ln 5d and the ligand orbitals can indirectly perturb the energy and intensity of the sharp f–f transitions.[25] Computational treatment of these states remains a challenge; however, it has become clear that they must be explicitly included in order to arrive at more accurate and quantitative descriptions of the electronic energy levels of lanthanoids.[26,27] Indeed, from comparative studies in sesquioxides (Ln_2O_3) the non-monotonic periodicity in their band gap energies was shown. La and Gd have no f bands in the band gap energy region, and their transitions are dominated by O 2p → Ln 5d states; in the first lanthanoids (Ce, Pr, and Nd) the fundamental band gap arises from transitions of Ln 4f → Ln 5d character; lastly, in the later lanthanoids (Pm–Tm) the transition occurs between O 2p → Ln 4f states. Similar conclusions were derived from an X-ray spectroscopic study by Altman *et al.*,[28] and their proposed qualitative band diagram is reproduced in Fig. 3b. These observed trends in the band gap energies in oxides were qualitatively followed in our study on $Ln_{10}S_{14}O$ (Fig. 3a, bottom) with a significant sub-bandgap photocurrent being detected. Although the cause may be a combination of structural defects and lanthanoid 4f states.[14] Nevertheless, given that the substitution of O^{2-} anions for softer S^{2-} changes the chemical environment and symmetry of the lanthanoids' coordination sphere, it would be of great interest to expand on these computational and spectroscopic studies to the full spectrum of lanthanoid oxysulphides and understand the degree of participation of the 4f orbitals in their electronic structures.

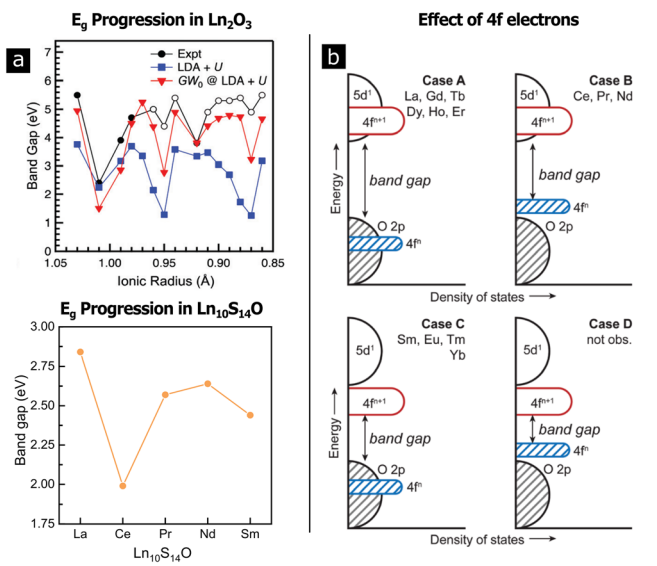

Fig. 3 (a) Top, band gap progression in Ln_2O_3. Reproduced with permission from ref. 28. Copyright 2016 by the Royal Society of Chemistry. Bottom, band gap progression in $Ln_{10}S_{14}O$ as a function of the lanthanoid cation; (b) qualitative band diagram of Ln_2O_3, reproduced with permission from ref. 28. Copyright 2016 by the Royal Society of Chemistry.

Thermodynamic stability and synthesizability

Generally, the synthesis of sulphides and oxysulphides of the trivalent lanthanoid ions is energetically demanding. This is owing to the lower affinity that the hard acids, Ln^{3+}, have for S^{2-} – a soft base –, as opposed to the O^{2-} hard bases that are part of most starting materials. The milder synthetic conditions (temperatures of *ca.* 300 °C) are suitable for colloidal nanoparticles of Ln_2O_2S, where high-boiling point coordinating solvents are used (like oleylamine and octadecene) in combination with the lanthanoid precursor and a sulphur source.[29] More recently thermal decomposition of single precursors, like thiocarbamates, has been used with great success.[20] However, in the solid state and for compositions with greater S : O ratios, temperatures between 600 and 1200 °C are required. Their syntheses involve a lanthanoid salt (*e.g.*, oxides and sulphates) and elemental sulphur, if reacting in a closed vessel,[15,30,31] or a sulphurizing agent (*e.g.* H_2S or CS_2) if the synthesis is carried under flow.[10,14]

Ln_2O_2S oxysulphides have been synthesized for the majority of the lanthanoids. However, reports on the properties of the pure-phase heavier members (Tb–Lu) are rare.[32–34] Similarly, the higher sulphur content members of the spectrum are mostly limited to the light rare earths (up to Gd). Despite their intriguing properties, there remains a large degree of uncertainty in the landscape of lanthanoid oxysulphides and the conditions required for their synthesis as the reports on the thermodynamics of these systems are scarce.[35–37] Even the most complete account, by Vaughan and White,[37] is qualitative in many aspects and limited to only a few oxysulphides and their polymorphs (as seen in Fig. 4). It is interesting to note how the region of existence of $Ln_{10}OS_{14}$ (the β polymorph) decreases along the lanthanoid series, matching our experimental observations of more challenging pure-phase synthesis of the heavier lanthanoids. It is possible that the increasing ionicity of the heavier lanthanoid trivalent cations makes bonding with the softer sulphide ligand an even higher thermodynamic uphill battle. Hence the need for calorimetric studies which could provide solid foundational grounds to understand the stability and synthesizability of the known oxysulphide phases quantitatively, and a tool to expand the realm of compositions and polymorphism.

The case of cerium

Among the published literature, there is a remarkable distinct photophysical behaviour in the cerium oxysulphides in comparison with the rest of the rare earths,[12,14] likely originating from a unique electronic structure. Most lanthanoids can attain multiple oxidation states, beyond the common +3.[38,39] In cerium, the +4 oxidation state is particularly easily attainable, and has indeed been identified in its own series of oxysulphides.[40–42] This proclivity to oxidation is responsible for stark colour changes in Ce_2O_2S when exposed to O_2.[29,43]

Published on 01 April 2024. Downloaded by University of California - Davis on 1/16/2025 7:42:10 PM.

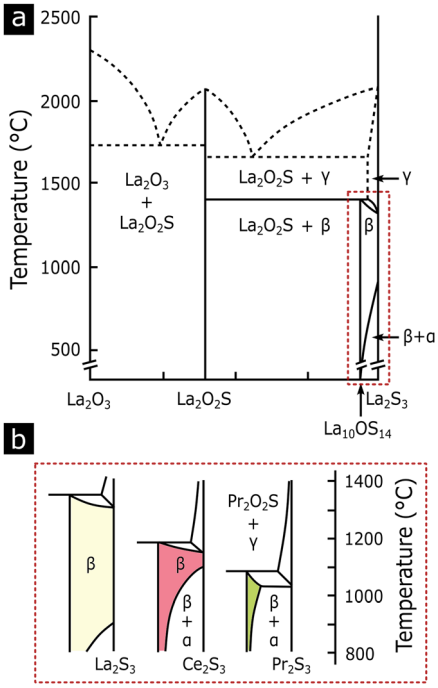

Fig. 4 (a) Compiled Ln–O–S phase diagram data for lanthanum; (b) magnification of the high-S content portion of the phase diagram showing differences between La, Ce, and Pr. The coloured regions correspond to the $Ln_{10}OS_{14}$ polymorph, the β phase. Adapted with permission from ref. 37. Copyright 1987 by the Materials Research Society.

However, it is yet unclear what determines the intrinsic distinction in cerium oxysulphides' optical properties compared with its congeners, in the absence of chemical changes. One such example is the similar band gap energies between Ce_2O_2S,[29] and $Ce_{10}OS_{14}$,[14] irrespective of the sulphur content. It is possible that the absorption onset is dominated by the dipole allowed 4f → 5d transitions in Ce^{3+} that appear as broad features centred at 500 nm.[44] Further spectroscopic measurements from the intermediate S-content oxysulphides would be instructive.

Conclusions and future outlook

Lanthanoid oxysulphides represent a large compositional space, where the sulphide content and lanthanoid identities can act as handles for targeted materials design. The entire sulphur spectrum exhibits multiple interesting structural and opto-electronic properties; yet, most research has focused on Ln_2O_2S oxysulphides. While certainly deserving of further investigations, we believe that the higher-sulphur-content-containing oxysulphides hold great untapped potential as multifunctional materials. This is because they combine the optical properties derived from the uniquely complex electronic structure of the lanthanoid ions with the tunability that a mixed-anion periodic solid can offer. As such, we envision that these oxysulphides could see wide ranging applications, from sulphur-involving batteries, in the case of $Ln_2O_2S_2$, for instance, to supports and local thermal sensors for catalysis under harsh environments. We hope this *Frontiers* article inspires further research into these exciting mixed-anion materials.

Conflicts of interest

There are no conflicts to declare.

Acknowledgements

JMV thanks the University of California, Davis for start-up funding. JMV also acknowledges the support from the Cottrell Scholars Program supported by the Research Corporation for Science Advancement (RCSA 26780), the Camille Dreyfus Teacher-Scholar Awards Program (TC-22-096-0), the Alfred P. Sloan Foundation award, as well as the support from the National Science Foundation through the Faculty Early Career Development Program (DMR-2044403).

References

1 J. J. Pitha, A. L. Smith and R. Ward, *J. Am. Chem. Soc.*, 1947, **69**, 1870–1871.
2 P. Liu, F. Wang, B. Yang and X. Chen, *Appl. Phys. A*, 2019, **125**(11).
3 I. Valsamakis and M. Flytzani-Stephanopoulos, *Appl. Catal., B: Environmental*, 2011, **106**(1–2), 255–263.
4 S. Tan and D. Li, *ChemCatChem*, 2018, **10**, 550–558.
5 C. Larquet, Y. Klein, D. Hrabovsky, A. Gauzzi, C. Sanchez and S. Carenco, *Eur. J. Inorg. Chem.*, 2019, 762–765, DOI: 10.1002/ejic.201801466.
6 J. Jiao, Y. Liu, H. Wang, X. Yin, M. Xing, X. Luo and Y. Tian, *J. Am. Ceram. Soc.*, 2020, **104**, 985–994.
7 W. Zheng, B. Sun, Y. Li and R. Wang, *ACS Appl. Nano Mater.*, 2021, **4**, 3922–3931.
8 Q. Zou, C. Marcelot, N. Ratel-Ramond, X. Yi, P. Roblin, F. Frenzel, U. Resch-Genger, A. Eftekhari, A. Bouchet, C. Coudret, M. Verelst, X. Chen, R. Mauricot and C. Roux, *ACS Nano*, 2022, **16**, 12107–12117.
9 M. Jia, X. Chen, R. Sun, D. Wu, X. Li, Z. Shi, G. Chen and C. Shan, *Nano Res.*, 2022, **16**, 2949–2967.
10 E. I. Sal'nikova, Y. G. Denisenko and O. V. Andreev, *Inorg. Mater.*, 2022, **58**, 516–524.
11 L. Meyniel, C. Boissiere, N. Krins and S. Carenco, *Langmuir*, 2023, **39**, 728–738.
12 C. Larquet, A.-M. Nguyen, E. Glais, L. Paulatto, C. Sassoye, M. Selmane, P. Lecante, C. Maheu, C. Geantet, L. Cardenas, C. Chanéac, A. Gauzzi, C. Sanchez and S. Carenco, *Chem. Mater.*, 2019, **31**, 5014–5023.
13 T. Schleid and F. Lissner, *J. Less-Common Met.*, 1991, **175**, 309–319.

This journal is © The Royal Society of Chemistry 2024

Published on 01 April 2024. Downloaded by University of California - Davis on 1/16/2025 7:42:10 PM.

14 B. A. Wuille Bille, A. C. Kundmann, F. E. Osterloh and J. M. Velázquez, *Chem. Mater.*, 2022, **34**, 7553–7562.
15 L. B. Mvélé, S. Sasaki, C. Latouche, P. Deniard, E. Janod, I. Braems, S. Jobic and L. Cario, *Inorg. Chem.*, 2023, **62**, 7264–7272.
16 P. Besançon, *J. Solid State Chem.*, 1973, **7**, 232–240.
17 X. Ou, X. Qin, B. Huang, J. Zan, Q. Wu, Z. Hong, L. Xie, H. Bian, Z. Yi, X. Chen, Y. Wu, X. Song, J. Li, Q. Chen, H. Yang and X. Liu, *Nature*, 2021, **590**, 410–415.
18 E. M. Chan, G. Han, J. D. Goldberg, D. J. Gargas, A. D. Ostrowski, P. J. Schuck, B. E. Cohen and D. J. Milliron, *Nano Lett.*, 2012, **12**, 3839–3845.
19 N. Pasberg, D. den Engelsen, G. R. Fern, P. G. Harris, T. G. Ireland and J. Silver, *Dalton Trans.*, 2017, **46**, 7693–7707.
20 B. Ward-O'Brien, E. J. Pickering, R. Ahumada-Lazo, C. Smith, X. L. Zhong, Y. Aboura, F. Alam, D. J. Binks, T. L. Burnett and D. J. Lewis, *J. Am. Chem. Soc.*, 2021, **143**, 21560–21566.
21 B. Ward-O'Brien, P. D. McNaughter, R. Cai, A. Chattopadhyay, J. M. Flitcroft, C. T. Smith, D. J. Binks, J. M. Skelton, S. J. Haigh and D. J. Lewis, *Nano Lett.*, 2022, **22**, 8045–8051.
22 M. Yang, J. Oró-Solé, J. A. Rodgers, A. B. Jorge, A. Fuertes and J. P. Attfield, *Nat. Chem.*, 2011, **3**, 47–52.
23 X. Chen and K. M. Ok, *Chem. Sci.*, 2022, **13**, 3942–3956.
24 J. L. Mason, H. Harb, J. E. Topolski, H. P. Hratchian and C. C. Jarrold, *Acc. Chem. Res.*, 2019, **52**, 3265–3273.
25 B. S. Zanella, S. B. Jones, H. S. Lee and R. D. Hancock, *Inorg. Chem.*, 2022, **61**, 4627–4638.
26 M. Mikami and S. Nakamura, *J. Alloys Compd.*, 2006, **408–412**, 687–692.
27 R. Gillen, S. J. Clark and J. Robertson, *Phys. Rev. B: Condens. Matter Mater. Phys.*, 2013, **87**(12), 125116.
28 A. B. Altman, J. I. Pacold, J. Wang, W. W. Lukens and S. G. Minasian, *Dalton Trans.*, 2016, **45**, 9948–9961.
29 C. Larquet, A. M. Nguyen, M. Avila-Gutierrez, L. Tinat, B. Lassalle-Kaiser, J. J. Gallet, F. Bournel, A. Gauzzi, C. Sanchez and S. Carenco, *Inorg. Chem.*, 2017, **56**, 14227–14236.
30 F. Lissner and T. Schleid, *Z. Naturforsch., B: J. Chem. Sci.*, 1992, **47**, 1614–1620.
31 T. Schleid and F. A. Weber, *Z. Kristallogr.*, 1998, **213**, 32.
32 Y. Abbas, J. Rossat-Mignod, F. Tcheou and G. Quezel, *Physica B+C*, 1977, **86–88**, 115–117.
33 X.-F. Zhang, H.-H. Zou, L.-W. Ding, X.-X. Deng, J.-J. Zheng, H.-F. Liu, Z.-M. Ye, S. Zhong, Z.-Y. Du, J. Zhang and C.-T. He, *Cell Rep. Phys. Sci.*, 2023, **4**(9), 101571.
34 P. Chen, B. Peng, Z. Liu, J. Liu, D. Li, Z. Li, X. Xu, H. Wang, X. Zhou and T. Zhai, *J. Am. Chem. Soc.*, 2024, **146**(9), 6053–6060.
35 R. J. Fruehan, *Metall. Trans. B*, 1979, **10**, 143–148.
36 M. Leskelä, *Thermochim. Acta*, 1985, **92**, 739–742.
37 C. M. Vaughan and W. B. White, *Mater. Res. Soc. Symp. Proc.*, 1987, **97**, 397–402.
38 M. Tricoire, N. Mahieu, T. Simler and G. Nocton, *Chem. – Eur. J.*, 2021, **27**, 6860–6879.
39 T. P. Gompa, A. Ramanathan, N. T. Rice and H. S. La Pierre, *Dalton Trans.*, 2020, **49**, 15945–15987.
40 P. J. Dugué, D. Carré and M. Guittard, *Acta Crystallogr., Sect. B: Struct. Crystallogr. Cryst. Chem.*, 1978, **34**, 3564–3568.
41 P. J. Dugué, D. Carré and M. Guittard, *Acta Crystallogr., Sect. B: Struct. Crystallogr. Cryst. Chem.*, 1979, **35**, 1550–1554.
42 W. Wichelhaus, *Angew. Chem., Int. Ed. Engl.*, 1978, **17**, 451–452.
43 C. Sourisseau, R. Cavagnat, R. Mauricot, F. Boucher and M. Evain, *J. Raman Spectrosc.*, 1997, **28**, 965–971.
44 J. Xu, S. Tanabe, A. D. Sontakke and J. Ueda, *Appl. Phys. Lett.*, 2015, **107**, 081903.
45 K. Momma and F. Izumi, *J. Appl. Crystallogr.*, 2008, **41**, 653–658.